Hindawi
Advances in Condensed Matter Physics
Volume 2020, Article ID 3407141, 9 pages
https://doi.org/10.1155/2020/3407141

Research Article

Ab Initio High-Pressure Study of Semiconductor-Metal Phase Transition of the Chalcogenide Compound $KPSe_6$

P. O. Jomo,[1] **C. O. Otieno**,[1] **and P. W. O. Nyawere**[2]

[1]*Department of Physics, Kisii University, P.O. Box 408, Kisii, Kenya*
[2]*Department of Physical and Biological Sciences, Kabarak University, P.O. Box, Private Bag 20157, Nakuru, Kenya*

Correspondence should be addressed to P. O. Jomo; phigrey@students.kisiiuniversity.ac.ke

Received 3 December 2019; Revised 10 March 2020; Accepted 30 March 2020; Published 1 May 2020

Academic Editor: Gayanath Fernando

We report the results of pressure-induced semiconductor-metal phase transition of the semiconducting chalcogenide compound $KPSe_6$ under high pressure using the ab initio methods. The ground-state energy calculations were performed within density functional theory and the generalized gradient approximation using the pseudopotential method with plane-wave basis sets. The projector augmented-wave (PAW) pseudopotentials were used in our calculation. The optimized lattice parameters were found from total energy calculations as 13 Bohr, 1.6 Bohr, and 1.8 Bohr for cell dimensions one, two, and three, respectively, which are in good agreement with experimental calculations. At zero pressure, the material portrayed a semiconducting property with a direct bandgap of ≈1.7 eV. As we subjected the material to pressure, the band gap was observed to reduce until it disappeared. The phase transition from the semiconductor to metal was found to occur at ~45 GPa, implying that the material underwent metallization as pressure was increased further.

1. Introduction

In the recent past, research on the effect of pressure on structural phase transformations and characteristics of materials by calculations from first principles have attracted much attention since they give an insight into the nature of solid-state theories [1, 2], and also assist in determining values of essential parameters for industrial applications [3]. For example, the structural, electrical, and optical properties of group III–V semiconducting compounds have been studied extensively [1, 3–5].

Most elements do undergo structural phase transitions as pressure is induced [6–9]. When a material is subjected to compressional forces, its electronic band structure changes [10, 11] which further results in a change in its structural properties [10, 12–14]. This often leads first to the formation of low-symmetry complex structures which at higher pressure then transform into high-symmetry close-packed structures [6, 8, 13]. Besides, the delocalization of bonding electrons under pressure reduces the differences between the chemical properties of the elements and their crystal structures [15]. As a result, numerous new allotropes of the elements have been discovered [16].

Structural studies of chalcogenides under high pressure up to 52 GPa have been carried out experimentally by using X-ray diffraction method [9]. For example, CaS, CaSe, and CaTe alkaline-earth chalcogenides undergo a structural phase transition at a pressure of 40 GPa, 38 GPa, and 33 GPa, respectively [9, 14]. The study of crystalline materials under pressure in material physics gives very important and useful material properties [1, 6, 9, 10, 12, 13, 17]. Subjecting a material to high pressure leads to a reduction of interatomic spacing which in turn affects the crystal structure and electronic orbitals [1, 18–23]. Likewise, high pressure can result in the formation of new material with different features from the initial material [24].

Chalcogenide glasses are based on selenium, tellurium, and the addition of other elements such as arsenic, germanium, antimony, gallium, and potassium [3, 25]. They are well known for their advantages, such as a wide transmittance range (1–12 μm) [3], low intrinsic losses in the mid-IR [26], low phonon energy [27], and the absence of free-carrier

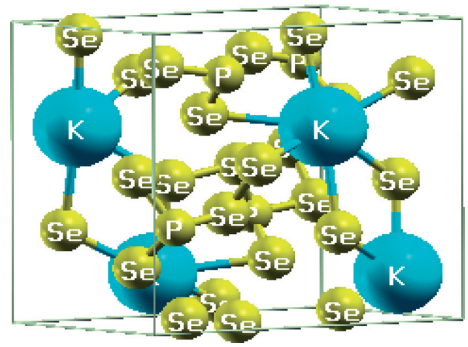

Figure 1: The optimized crystal structure of $KPSe_6$ at zero pressure as viewed using the crystalline and molecular structure visualization program (XCrySDen). The obtained crystal structure is orthorhombic and is in good agreement with the general crystal structure [32].

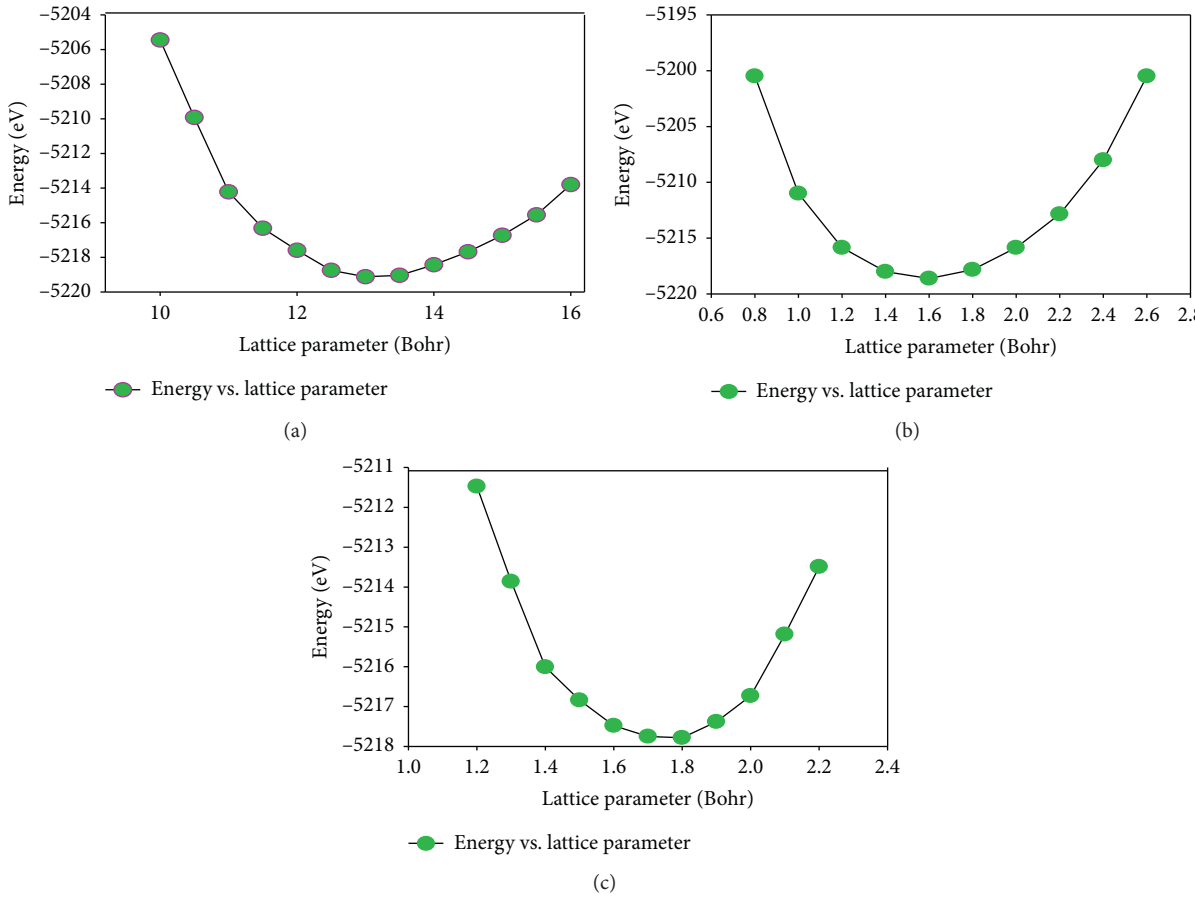

Figure 2: (a) A convergence curve for cell dimension one which gives ~13.0 Bohr, (b) the optimized value for cell dimension two is ~1.6 Bohr, and (c) the optimized value for cell dimension three is ~1.8 Bohr. These optimized values were used in subsequent calculations.

effects [3, 28–30]. $KPSe_6$ as a chalcogenide has attracted much interest because of its promising abilities in technological applications such as thin films and optical fibers [3, 25, 27, 30, 31]. $KPSe_6$ crystallizes in the polar orthorhombic space group $Pca2_1$ [3, 26, 32]. This compound is a semiconductor at zero pressure with a direct bandgap of 1.883 eV [3, 26, 31, 33]. We aimed at investigating the behavior of $KPSe_6$ under very high pressure.

We arrange this paper in the following order: we explain the details of the calculation in Section 2, Section 3 discusses the results, and conclusions are in Section 4.

2. Computational Details

The study was done using the density functional theory (DFT) [34] by employing for the exchange-correlation

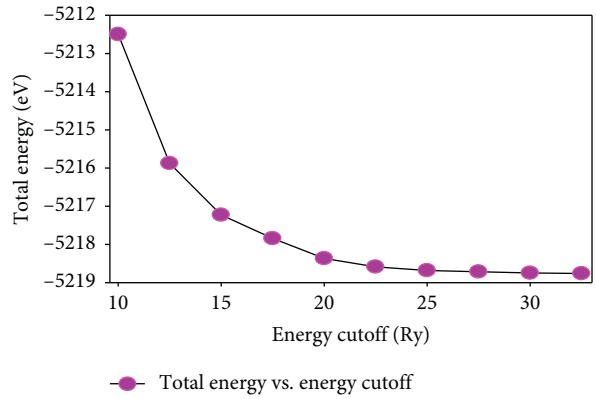

Figure 3: A representative convergence curve for total energy versus kinetic energy cutoff. The optimized energy cutoff at the minima was ~25 Ry as shown.

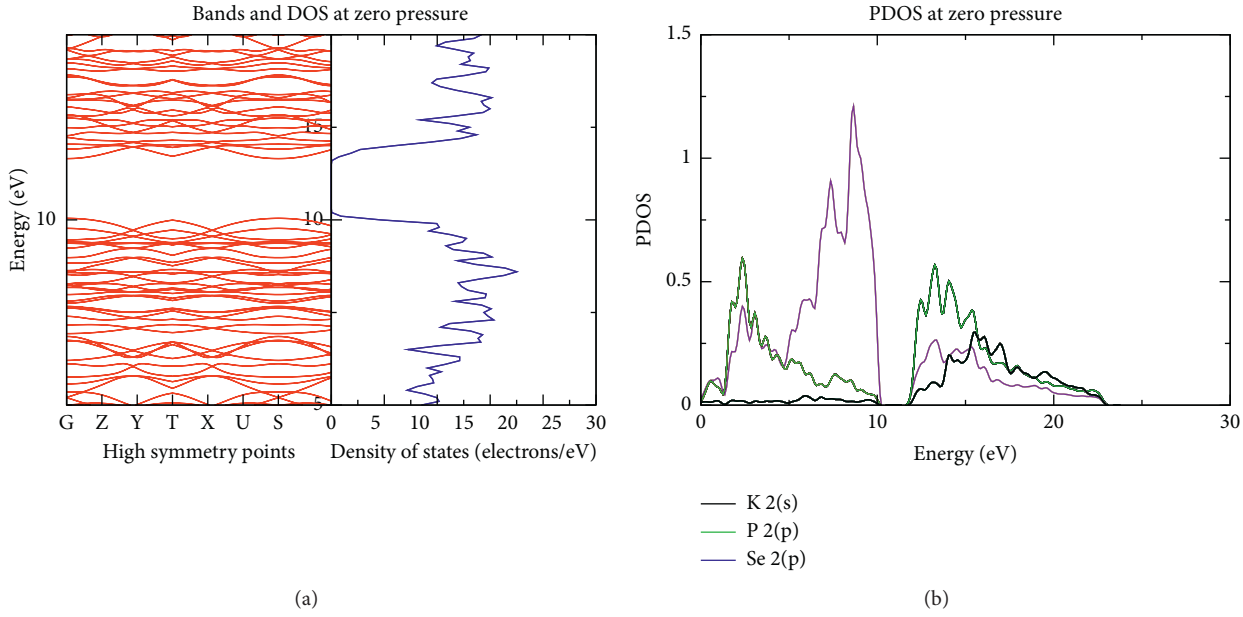

Figure 4: (a) The electronic band structure and the density of states. The band structure and density of states show a very close similarity as seen above. (b) The curves represent the partial density of states and how each atom contributes to either the valance band or conduction band. It can be noted that Se 2(p) states contribute more to the valence band compared potassium and selenium, while P 2(p) states contribute more to the conduction band.

functional, the generalized gradient approximation of Perdew–Burke–Ernzerhof [34–36] based on Plane Wave self-consistent field (PWscf) and Ultrasoft pseudopotential (USPP) method. Pressure increase was implemented as follows: starting with the relaxed unit cell, we modified the input file whereby we changed the "calculation" type from "scf" to "vc-relax" and then introduced two new segments; the first segment is called "&ions' while the second one is called '&cell." Under the first segment, the ion dynamics were set to damp while under the second segment, we entered the target pressure (Kbar) that we wanted to subject our cell to [35]. The new atomic positions obtained were then used to calculate the electronic structure properties of $KPSe_6$ as at that pressure. The ab initio calculations are implemented in the Quantum Espresso simulation package [36], and pseudopotentials were taken from the Quantum Espresso database. For pseudopotentials, the valence electrons are 2s for K, 2p for P, and 2p for Se. The valence wave functions were expanded in a plane wave basis set truncated at a kinetic energy of 25 Ry (340 eV). At ambient conditions, $KPSe_6$ crystallizes in the polar orthorhombic space group $Pca2_1$ [3, 26, 32]. The structure has three species of atoms as potassium K, phosphorous P, and selenium Se. The primitive unit cell of the chalcogenide compound $KPSe_6$ has a total of 32 atoms: 4 potassium atoms, 4 phosphorous atoms, and 24 selenium atoms. Figure 1 shows the optimized crystal structure of $KPSe_6$.

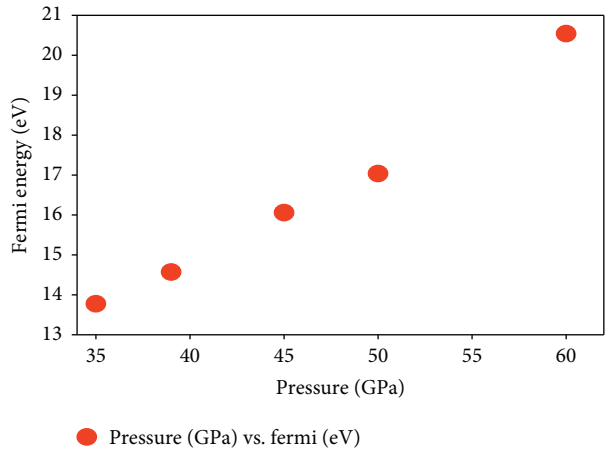

Figure 5: Induced pressure dependence of the Fermi energy. There is a continued increase in Fermi energy with increased pressure, provided the structure has not undergone distortion [6, 41].

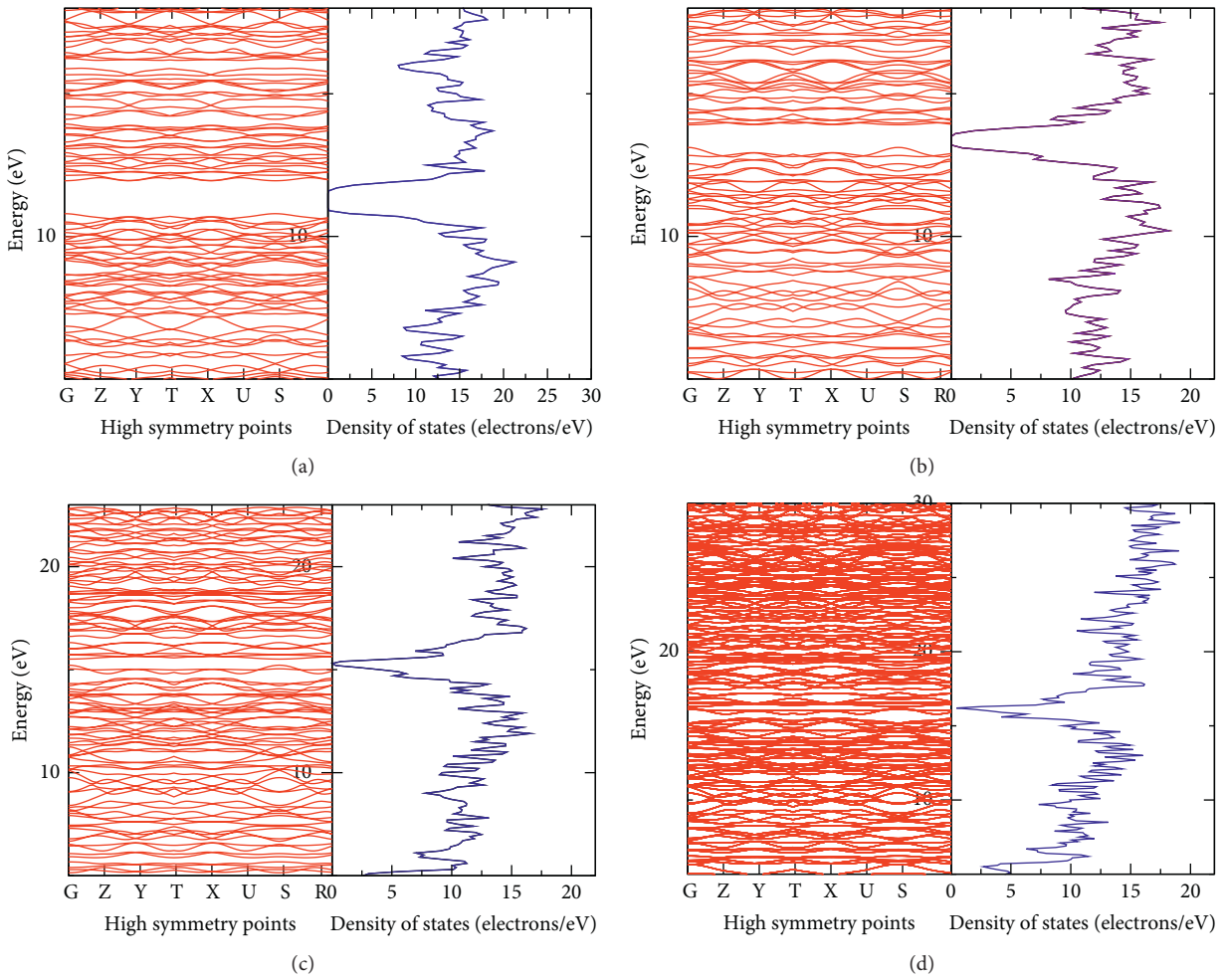

Figure 6: Calculated pressure-dependent band structures and density of states for the compound $KPSe_6$ at (a) 20 GPa, (b) 30 GPa, (c) 40 GPa, and (d) 45 GPa. The bandgaps are ~1.18 eV at 20 GPa (a), ~1.05 eV at 30 GPa (b), ~0.50 eV at 40 GPa (c), and 0.00 eV at 45 GPa (d).

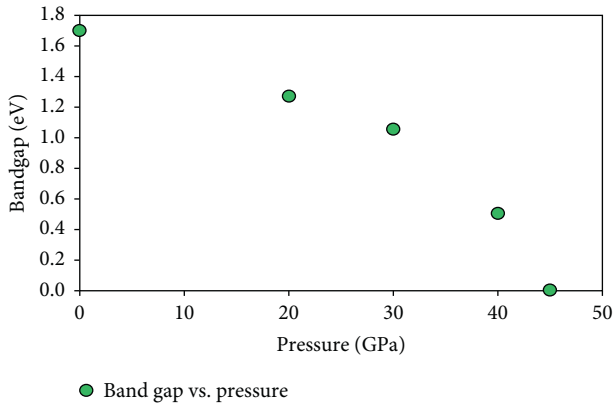

Figure 7: A plot of the calculated band gaps versus the pressure of the chalcogenide compound $KPSe_6$.

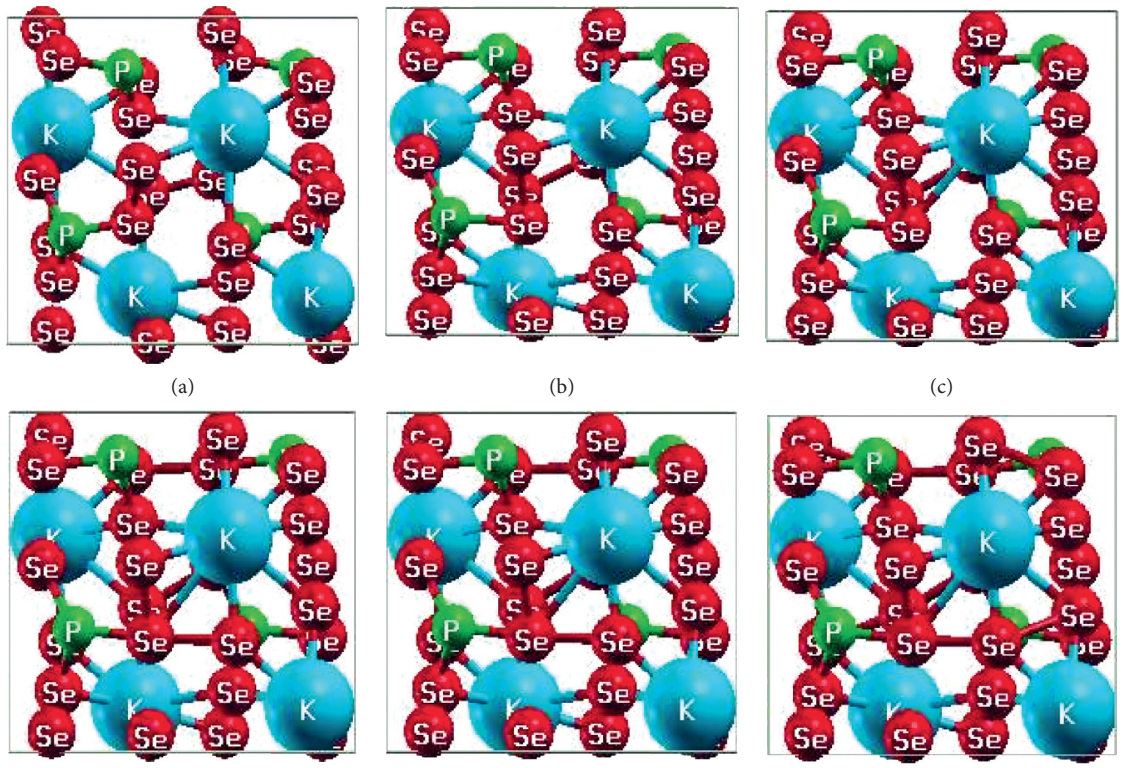

Figure 8: Crystal structures for $KPSe_6$ at pressure (a) 0 GPa, (b) 20 GPa, (c) 30 GPa, (d) 40 GPa, (e) 45 GPa, and (f) 50 GPa, respectively, as viewed using crystalline and molecular structure visualization program (XCrySDen). The crystal structure remained undistorted as pressure was increased. This implies that the structure remained stable and that there was no structural phase transition.

Table 1: Shows a structural analysis of KPSe6 in terms of bond lengths and bond angles at various pressure intervals.

Pressure (GPa)	KPSe6 structure analysis			
	Bond length (Å)			Bond angle (°)
	K-Se	P-Se	Se-Se	K-Se-P
0	2.8002	1.9284	1.9703	83.030
20	2.8460	2.1322	2.2821	85.293
30	2.7130	2.0643	2.2234	84.275
40	2.6131	2.0090	2.1729	83.822
45	2.5707	1.9858	2.1526	84.094
50	2.5317	1.9627	2.1290	84.285

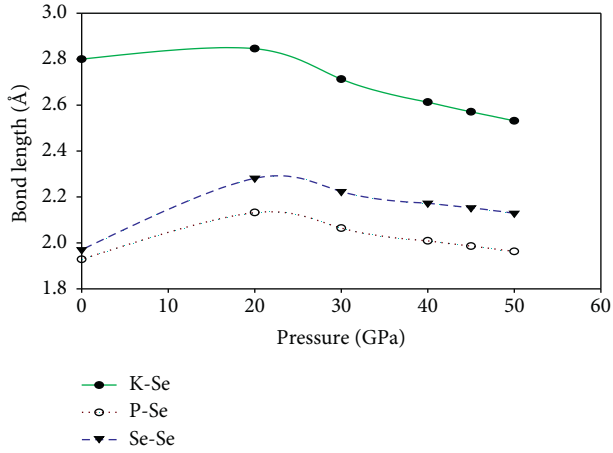

Figure 9: A plot of pressure versus bond lengths of the atoms. The green curve shows the variation of the bond length between potassium and selenium while the blue curve is for the phosphorous-selenium bond lengths, and the maroon curve shows the variation of the bond length between one selenium atom and another selenium atom. It was observed the bond length increased up to 20 GPa after which it reduced with further application of pressure.

3. Results and Discussion

3.1. Structural Optimization. In this section, we report the graphical representation of the optimized lattice parameters and kinetic energy cutoff (ecut) for our chalcogenide compound $KPSe_6$. The following graphs of Figure 2 represent how the optimized lattice parameters were obtained. The minima in the graphs represent the ground-state energy which corresponds to the accurate parameter to be used for the calculations.

The ground-state calculation for the optimized kinetic energy cutoff (ecut) was performed, and the graph is plotted as shown in Figure 3. The kinetic energy cutoff optimized value was ~25 Ry. This was the value used for the rest of the calculations.

3.2. Electronic Structure Properties. Calculations of the band structure, partial density of states, and density of states of the compound $KPSe_6$ are here reported. In order to determine the band structure properties, we used the following high symmetry points of Γ(0,0,0), X(1/2,0,0), Y(0,1/2,0), Z(0,0,1/2), T(0,1/2,1/2), U(1/2,0,1/2), S(1/2,1/2,0), and R(1/2,1/2,1/2) [16,37,38]. A direct bandgap of ~1.7 eV was obtained at zero pressure and the gap formed around the T-symmetry. This result is in agreement with the experimental value of 1.883 eV [3, 26, 37, 39] and is within the error bar range [37]. The underestimation is caused by the occupied states being lower in energy as compared to the unoccupied states [39, 40]. The bands and curves for the density of states for this compound are as presented in Figure 4.

3.3. Pressure-Induced Phase Transition. It is established that the bandgap of a material depends on the magnetic field, temperature, and pressure [39]. We examined how pressure affects the bandgap. According to Gulyamov [17, 23, 39], the pressure band gap relation is given by

$$E_g(P) = E_g(0) - \beta P, \tag{1}$$

where β represents the pressure coefficient which defines the shift in the position of the valence and conduction bands with variation in pressure [1, 18]. The Fermi level pressure dependence is given by [39]

$$E_F(P,T) = \frac{E_g(P)}{2} + \frac{3}{4}KT\ln\frac{m_h}{m_e}, \tag{2}$$

where E_F represents the Fermi energy, T is the absolute temperature, E_g gives the energy gap, m_e^* is the mass of an electron, and m_h^* is the mass of the hole. A graph showing the relationship between Fermi energy and pressure is as shown in Figure 5.

On inducing pressure, the number of charge carriers with respect to the density of state increased which in turn enhanced the availability of more electrons responsible for electrical conductivity [17, 42, 43]. As we introduced more pressure, there was an overlap between the valence band and the conduction band which was attributed to the broadening of the bandwidth of the 2s and 2p atomic orbital [20]. This was because of their strong interaction with neighboring atoms that created wider bands than the energy gap, thus availing electrons to the conduction band [41]. The phase transition from the semiconductor to metal was found to occur at ~45 GPa. Therefore, it was an indication that pressure can lead to the semiconductor-metal transition [42]. The changes in the band structure and density of state at different pressure in relation to Fermi energy are described using Figure 6.

The variation of bandgaps for pressure calculations was also plotted as shown in Figure 7.

The crystal structure was stable and not distorted at high pressure; this showed that the material can withstand high compressional forces and thus can be used for various high-pressure industrial applications. The crystal structures at various pressures are as shown in Figure 8.

The bond lengths and bond angles were investigated as well at various pressure intervals using crystalline and molecular structure visualization program (XCrySDen). It

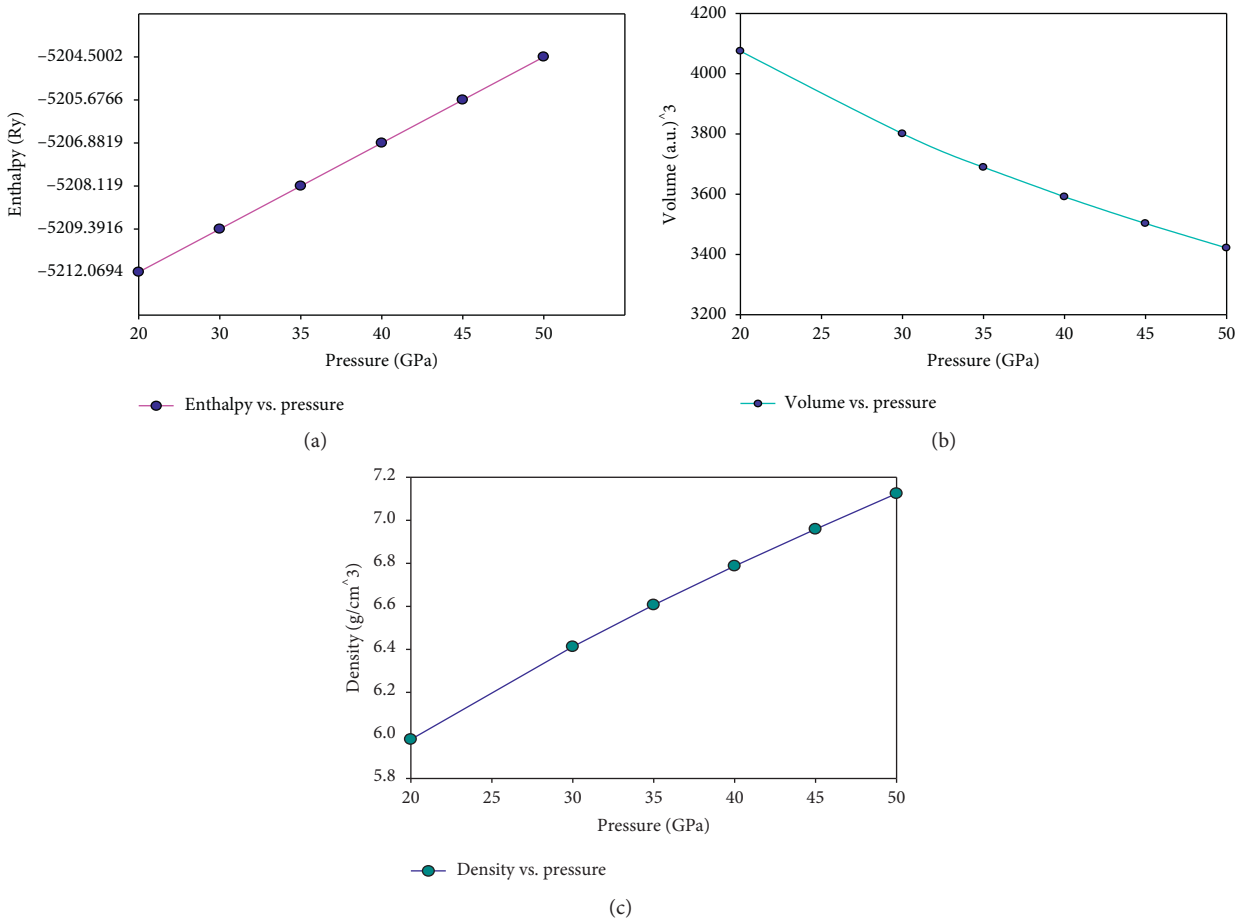

Figure 10: (a) A study on the effect of pressure on the enthalpy of the material. Pressure and enthalpy of the compound were found to be directly proportional. (b). A plot of the volume of the crystal against pressure. An inverse relationship was obtained as shown above. (c). A plot of the calculated density of the compound versus pressure. As more pressure was introduced into the system, the density of $KPSe_6$ increased as well. This implies that the stability of the chalcogenide compound $KPSe_6$ improved as pressure increased [17].

was observed that the bond lengths reduced as more pressure was induced while the bond angles decreased and then increased as from 40 GPa as shown in Table 1 and Figure 9.

The stability of the material is supported by the pressure-dependent study of band structures of $KPSe_6$ with respect to its enthalpy, volume, and density as calculated and analyzed in Figures 10(a)–10(c).

4. Conclusion

We have performed an ab initio theoretical and computational study of the chalcogenide compound $KPSe_6$. The structural and electronic properties of the chalcogenide compound were investigated under high pressure. Results show that the volume and energy gap for this material decrease while the enthalpy, Fermi energy, and density increase as we increase pressure. This shows the conductivity of this material increases with increasing pressure. From these calculations, the bands of the chalcogenide $KPSe_6$ overlap at a pressure of ~45 GPa. This implies that the material has undergone a semiconductor-metal transformation with a potential application to high pressure.

Data Availability

The KPSe6 input and output data used to support the findings of this study are available from the corresponding author upon request.

Conflicts of Interest

The authors declare no conflicts of interest.

Acknowledgments

The authors wish to thank the CHPC for availing computational resources and our collaborator Mr. Agora Jared for his informative contributions in support of this research.

References

[1] A. Bouhemadou, R. Khenata, F. Zegrar, M. Sahnoun, H. Baltache, and A. H. Reshak, "Ab initio study of structural, electronic, elastic and high pressure properties of barium chalcogenides," *Computational Materials Science*, vol. 38, no. 2, pp. 263–270, 2006.

[2] M. Bilal, M. Shafiq, I. Ahmad, and I. Khan, "First principle studies of structural, elastic, electronic and optical properties of Zn-chalcogenides under pressure," *Journal of Semiconductors*, vol. 35, no. 7, Article ID 072001, 2014.

[3] J. I. Jang, A. S. Haynes, F. O. Saouma, C. O. Otieno, and M. G. Kanatzidis, "Broadband studies of the strong mid-infrared nonlinear optical responses of KPSe_6," *Optical Materials Express*, vol. 3, no. 9, p. 1302, 2013.

[4] Hummer, 2003, iAb initioi study of anthracene under high pr.pdf.

[5] Z. Ma, K. Wu, R. Sa, Q. Li, and Y. Zhang, "Ab initio study of elasticity, piezoelectricity, and nonlinear optical performance in monoclinic NaAsSe2," *Journal of Alloys and Compounds*, vol. 568, pp. 16–20, 2013.

[6] G. Parthasarathy and E. S. R. Gopal, "Effect of high pressure on chalcogenide glasses," *Bulletin of Materials Science*, vol. 7, no. 3-4, pp. 271–302, 1985.

[7] R. Thangavel, G. Prathiba, B. Anto Naanci, M. Rajagopalan, and J. Kumar, "First principle calculations of the ground state properties and structural phase transformation for ternary chalcogenide semiconductor under high pressure," *Computational Materials Science*, vol. 40, no. 2, pp. 193–200, 2007.

[8] T.-L. Huang and A. L. Ruoff, "High-pressure-induced phase transitions of mercury chalcogenides," *Physical Review B*, vol. 31, no. 9, pp. 5976–5983, 1985.

[9] Z. Charifi, H. Baaziz, F. E. H. Hassan, and N. Bouarissa, "High pressure study of structural and electronic properties of calcium chalcogenides," *Journal of Physics: Condensed Matter*, vol. 17, no. 26, pp. 4083–4092, 2005.

[10] A. M. Hao, X. C. Yang, Z. M. Gao, X. Liu, Y. Zhu, and R. P. Liu, "First-principles investigations on structural and elastic properties of CaX (X=S, Se and Te) under high pressure," *High Pressure Research*, vol. 30, no. 2, pp. 310–317, 2010.

[11] N. Benkhettou, D. Rached, and M. Rabah, "Ab-initio calculation of stability and structural properties of cadmium chalcogenides CdS, CdSe, and CdTe under high pressure," *Czechoslovak Journal of Physics*, vol. 56, no. 4, pp. 409–418, 2006.

[12] H. Khachai, R. Khenata, A. Haddou et al., "First-principles study of structural, electronic and elastic properties under pressure of calcium chalcogenides," *Physics Procedia*, vol. 2, no. 3, pp. 921–925, 2009.

[13] P. Bhardwaj, S. Singh, and N. Gaur, "Structural and elastic properties of barium chalcogenides (BaX, X=O, Se, Te) under high pressure," *Open Physics*, vol. 6, no. 2, 2008.

[14] P. Bhardwaj, S. Singh, and N. K. Gaur, "Phase transition, mechanical properties and stability of strontium chalcogenides under high pressure," *Journal of Molecular Structure: THEOCHEM*, vol. 897, no. 1–3, pp. 95–99, 2009.

[15] T. Luty and C. J. Eckhardt, "General theoretical concepts for solid state reactions: quantitative formulation of the reaction cavity, steric compression, and reaction-induced stress using an elastic multipole representation of chemical pressure," *Journal of the American Chemical Society*, vol. 117, no. 9, pp. 2441–2452, 1995.

[16] W. Steurer, "Crystal structures of the elements," in *Reference Module in Materials Science and Materials Engineering*, Elsevier, Amsterdam, Netherlands, 2017.

[17] D. Olguín, A. Cantarero, C. Ulrich, and K. Syassen, "Effect of pressure on structural properties and energy band gaps of γ-InSe," *Physica Status Solidi (b)*, vol. 235, no. 2, pp. 456–463, 2003.

[18] Z. Zhao, H. Zhang, H. Yuan et al., "Pressure induced metallization with absence of structural transition in layered molybdenum diselenide," *Nature Communications*, vol. 6, no. 1, p. 7312, 2015.

[19] D. Varshney, N. Kaurav, R. Kinge, and R. K. Singh, "Pressure induced phase transition (B1–B2) and elastic properties in alkaline earth BaX (X = S, Se and Te) chalcogenides: phase transitions," *Phase Transitions*, vol. 81, no. 1, 2008.

[20] Z.-H. Chi, "Pressure-induced metallization of molybdenum disulfide," *Physical Review Letters*, vol. 113, no. 3, Article ID 036802, 2014.

[21] G. Itkin, G. R. Hearne, E. Sterer, M. P. Pasternak, and W. Potzel, "Pressure-induced metallization of ZnSe," *Physical Review B*, vol. 51, no. 5, pp. 3195–3197, 1995.

[22] S. Yamaoka, O. Shimomura, H. Nakazawa, and O. Fukunaga, "Pressure-induced phase transformation in BaS," *Solid State Communications*, vol. 33, no. 1, pp. 87–89, 1980.

[23] F. J. Manjon, I. Tiginyanu, and V. Ursaki, Eds., *Pressure-Induced Phase Transitions in AB2X4 Chalcogenide Compounds*, Springer, Vol. 189, Berlin, Germany, 2014.

[24] M. Durandurdu and D. A. Drabold, "Simulation of pressure-induced polyamorphism in a chalcogenide glass GeSe 2," *Physical Review B*, vol. 65, no. 10, 2002.

[25] G. E. Snopatin, V. S. Shiryaev, V. G. Plotnichenko, E. M. Dianov, and M. F. Churbanov, "High-purity chalcogenide glasses for fiber optics," *Inorganic Materials*, vol. 45, no. 13, pp. 1439–1460, 2009.

[26] I. Chung and M. G. Kanatzidis, "Metal chalcogenides: a rich source of nonlinear optical materials," *Chemistry of Materials*, vol. 26, no. 1, pp. 849–869, 2014.

[27] J. M. Léger, "Chalcogenides and pnictides of cerium and uranium under high pressure," *Physica B: Condensed Matter*, vol. 190, no. 1, pp. 84–91, 1993.

[28] I. Chung, M.-G. Kim, J. I. Jang, J. He, J. B. Ketterson, and M. G. Kanatzidis, "Strongly nonlinear optical chalcogenide thin films of APSe6 (A=K, Rb) from spin-coating," *Angewandte Chemie*, vol. 123, no. 46, pp. 11059–11062, 2011.

[29] I. Chung, J. Do, C. G. Canlas, D. P. Weliky, and M. G. Kanatzidis, "APSe6(A = K, Rb, and Cs): polymeric selenophosphates with reversible phase-change properties," *Inorganic Chemistry*, vol. 43, no. 9, pp. 2762–2764, 2004.

[30] J. Lucas, "Infrared glasses," *Current Opinion in Solid State and Materials Science*, vol. 4, no. 2, pp. 181–187, 1999.

[31] F. Liang, L. Kang, Z. Lin, and Y. Wu, "Mid-Infrared nonlinear optical materials based on metal chalcogenides: structure-property relationship," *Crystal Growth & Design*, vol. 17, no. 4, pp. 2254–2289, 2017.

[32] K. Persson, *Materials Data on KPSe6 (SG:29) by Materials Project-LBNL Materials Project*, Lawrence Berkeley National Laboratory (LBNL), Berkeley, CA, USA, 2014.

[33] I. Chung, M.-G. Kim, J. I. Jang, J. He, J. B. Ketterson, and M. G. Kanatzidis, "Strongly nonlinear optical chalcogenide thin films of APSe6 (A=K, Rb) from spin-coating," *Angewandte Chemie International Edition*, vol. 50, no. 46, pp. 10867–10870, 2011.

[34] D. S. Sholl and J. A. Steckel, *Density Functional Theory—A Practical Introduction*, Wiley, Hoboken, NJ, USA, 2009.

[35] "pw_user_guide.pdf.".

[36] P. Giannozzi, S. Baroni, N. Bonini et al., "Quantum espresso: a modular and open-source software project for quantum simulations of materials," *Journal of Physics: Condensed Matter*, vol. 21, no. 39, p. 395502, 2009.

[37] P. Mori-Sánchez, A. J. Cohen, and W. Yang, "Localization and delocalization errors in density functional theory and implications for band-gap prediction," *Physical Review Letters*, vol. 100, no. 14, Article ID 146401, 2008.

[38] "Condensed matter-why does density functional theory (DFT) underestimate bandgaps?," Physics Stack Exchange, https://physics.stackexchange.com/questions/176419/why-does-density-functional-theory-dft-underestimate-bandgaps.

[39] G. Gulyamov, U. I. Erkaboev, and A. G. Gulyamov, "Influence of pressure on the temperature dependence of quantum oscillation phenomena in semiconductors," *Advances in Condensed Matter Physics*, vol. 2017, Article ID 6747853, 6 pages, 2017.

[40] Y. Liu-Xiang, Z. Jing-Geng, Y. Yong, L. Feng-Ying, Y. Ri-Cheng, and J. Chang-Qing, "Metallization of Cu 3 N semiconductor under high pressure," *Chinese Physics Letters*, vol. 23, no. 2, pp. 426-427, 2006.

[41] H. Tups, A. Otto, and K. Syassen, "Pressure dependence of the d-band to Fermi-level excitation threshold in silver," *Physical Review B*, vol. 29, 1984.

[42] P. K. Jha, U. K. Sakalle, and S. P. Sanyal, "High pressure structural phase transition IN alkaline earth chalcogenides," *Journal of Physics and Chemistry of Solids*, vol. 59, no. 9, pp. 1633–1637, 1998.

[43] C. J. Pickard and R. J. Needs, "High-pressure phases of silane," *Physical Review Letters*, vol. 97, no. 4, Article ID 045504, 2006.